

Investigation of electrical and dielectric properties of "modified" iron titanates

M A Madare and S V Salvi*

ICLES' M. J. College of Arts, Science and Commerce,
Sector 9A, A. Roye Road, VASHI, New Mumbai-400 703, India

*Department of Physics, Institute of Science
15, Madame Cama Road, Mumbai-400 032, India

E-mail : director.isc.mum@gens.vsnl.net.in

Abstract : Iron titanate is a pseudobrookite and exhibits spin glass behaviour, thermal cracking, magnetic texture, high resistivity and many other interesting properties. Hence polycrystalline iron titanate has multifaceted applications. This communication presents synthesis and investigation of electrical resistivity as a function of temperature and dielectric behaviour as a function of temperature as well as frequency (relaxation spectra) of "pure" and "modified" iron titanates.

"Pure" iron titanate is synthesized by usual standard ceramic method using A. R. grade oxides. In "modified" iron titanates, the ionic pair of "lithium and aluminium" is incorporated by the ceramic technique. The percentage of lithium and aluminium in each sample is determined by chemical analysis using ICAP technique. The single phase formation is confirmed by XRD technique and structural information is obtained using XRD and FTIR techniques. Structurally, all samples remain pseudobrookite having orthorhombic cell.

The analysis of relaxation spectra establishes the presence of space-charge, which decreases on incorporation of "LiAl" pair. The changes in resistivity, dielectric constant, dielectric loss are discussed and analysed on the basis of doping, impurity compensation and grain texture.

Keywords : Pseudobrookite, "LiAl" -substitution, electrical and dielectric properties

PACS Nos. 72.80.Ga, 77.22.-d

1. Introduction

A solid state reaction between Fe_2O_3 and TiO_2 forms the very stable phase Fe_2TiO_5 [1]. The presence of Fe^{2+} ion is not observed in this phase [2]. Electrically, it is an n-type of semiconductor [3]. However, this is mainly due to random distribution of Fe^{3+} and Ti^{4+} ions [$(\text{Fe}^{3+}_{0.67}\text{Ti}^{4+}_{0.33})_4(\text{Fe}^{3+}_{1.33}\text{Ti}^{4+}_{0.67})_8$] among two octahedral sites (viz. 8f and 4c) where Ti^{4+} ion acts as donor. This compound has been investigated extensively for its magnetic spin glass behaviour [4-7]. The antiferromagnetic order in this compound is rendered short range by Ti layers and the compound has spin glass transition at 53 K [8]. The antiferromagnetic order is finally destroyed above 650 K [9]. Recently, the compound has been investigated for large thermal expansion anisotropy [10] thermodynamic equilibrium [11] and crystallographic texture [12]. This pseudobrookite exists in a orthorhombic or monoclinic phase [13]. The compound has also been used as photocatalyst [14], photoelectrode for electrolysis of water [15, 16]. Overall one gets an impression

that this compound has the potential of a wide range of applications.

This has encouraged us to pursue systematic investigation of its electrical, dielectric and magnetic properties. Also, the effect of LiAlH_4 , which is primarily known as reducing agent [17], on Fe_2TiO_5 is investigated. This paper reports the synthesis and electrical properties of Fe_2TiO_5 and its LITHIATED version. These characteristics would increase the range of the applicability of the compound.

2. Experimental

Fe_2TiO_5 was prepared by calcinating a mixture of fine powders of A.R. grade Fe_2O_3 and TiO_2 at 1000°C for 24 hours followed by homogenizing in an agate mortar and again calcinating at 1000°C for 24 hours. Powdered sample was used for X-ray powder diffraction. For "Lithiation", this prepared Fe_2TiO_5 was taken, x-mole of LiAlH_4 was added (where $x = 0.25; 0.50; 0.75$ and 1.00) and mixing thoroughly, it was calcinated at 1000°C for 24 hours. The samples are labelled and hereafter referred to as $S_{00}; S_{25};$

* Corresponding Author

S_{50} ; S_{75} and S_{100} respectively. The presence and quantity of lithium and aluminium in these samples was confirmed by chemical analysis using Inductively Coupled Argon Plasma (ICAP) technique. The residue is observed to be 0.10; 0.20; 0.30 and 0.40 mole of LiAl containing Li : Al in 1 : 1 ratio.

Dielectric constant (K') and dielectric loss (K'') are determined by using LCR-Q meter at an internal frequency 1 kHz by measuring the capacity of the parallel plate capacitor with pellet of sample as a dielectric medium; within the range of temperature 300 K – 600 K. Also, K' and K'' are determined at room temperature in the range of 10 kHz – 1000 kHz using an auto-computing digital LCR-Z meter (4277 A Hewlett Packard). The d.c. resistivity is measured by using the two probe method in the temperature range from room temperature to 600 K.

3. Results and discussion

The K' and K'' of S_{00} ; S_{25} ; S_{50} ; S_{75} and S_{100} have been calculated by using relation

$$\epsilon = Ct / A; K' = \epsilon / \epsilon_0; K'' = K' \tan \delta;$$

where $\tan \delta$ is the loss factor and C is the capacitance, t is the thickness of the pellet and A is the surface area of the pellet.

The resistivity (ρ) has been determined from measured resistance (R) of the sample by following equation

$$\rho = R \cdot A / t,$$

where A is the cross-sectional area of the pellet and also of the electrode and t is the pellet thickness. The conductivity (σ) is then

$$\sigma = 1 / \rho.$$

3.1 Dielectric characteristics at room-temperature :

The dielectric constant (K') and dielectric loss (K'') measured at room temperature and at 1 kHz are given in Table 1. Also, given in the table are two ratios viz [$K'_{10\text{ kHz}} / K'_{1\text{ kHz}}$] and [$K''_{10\text{ kHz}} / K''_{1\text{ kHz}}$]. Both the ratios are much smaller than unity except for S_{25} which is explained later by relaxation spectra. This indicates the presence of space-charge and the relaxation frequency of space-charge well below 10 kHz. The dielectric constant ranges from 200 to 500. These values are much smaller when compared

Table 1. Dielectric constant (K') and dielectric loss (K'') at room temperature at 1 kHz and 10 kHz. and conductivity (σ) at room temperature at 10 kHz.

Sample	S_{00}	S_{25}	S_{50}	S_{75}	S_{100}
$K'_{1\text{ kHz}}$	389	214	470	247	228
$K'_{10\text{ kHz}} / K'_{1\text{ kHz}}$	0.27	0.74	0.09	0.23	0.10
$K''_{1\text{ kHz}}$	957	45	>1000	92	55
$K''_{10\text{ kHz}} / K''_{1\text{ kHz}}$	0.09	4.38	0.02	0.39	0.11
Conductivity (σ) at 10kHz	5.67	6.33	4.04	2.74	1.47

to a ferroelectric material like BaTiO_3 [18] and relaxor like $\text{Pb}(\text{Mg}_{1/3}, \text{Nb}_{2/3})\text{O}_3$ [19]. Hence, the contribution of dipolar as well as interfacial polarization is small in these samples.

The plots of K' , K'' at 1 kHz and 10 kHz and conductivity at 10 kHz as function of LiAl content are given in Figures 1 and 2. All the plots are dome shaped, maxima correspond to $0.1 < x < 0.2$ where x is actual LiAl percentage mole content in the formula of the sample. Once again it indicates that the changes are due to interfacial polarization *i.e.* space-charge [20]. In this connection, it may be noted that S_{00} possesses a short range antiferromagnetic order [8]. Initially, the incorporation of LiAl

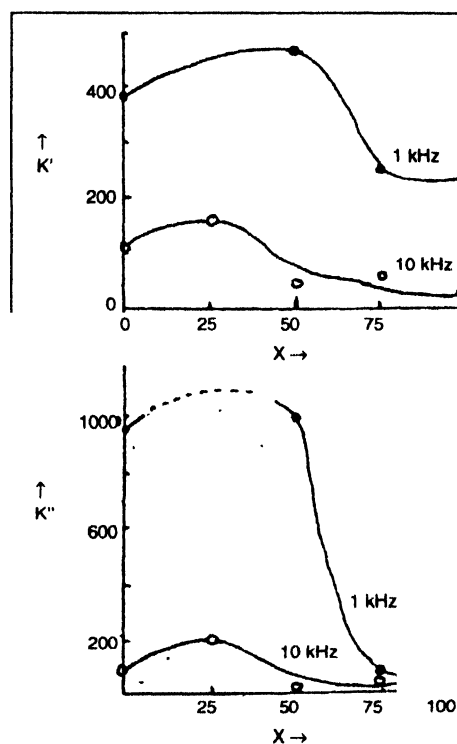


Figure 1. A plot of dielectric constant (K') vs mole percentage of LiAl (X) at 1 kHz and 10 kHz at room temperature and dielectric loss (K'') vs mole percentage of LiAl (X) at 1 kHz and 10 kHz at room temperature.

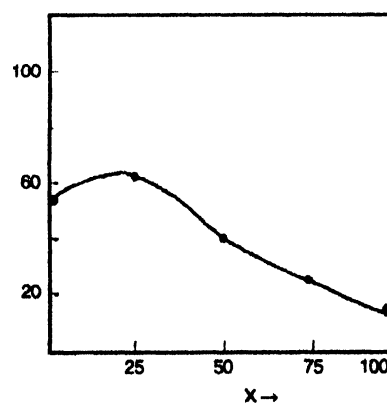


Figure 2. A plot of conductivity (σ) at 10 kHz vs mole percentage of LiAl (X) at 1 kHz and 10 kHz at room temperature.

pair may partly destroy antiferromagnetic order. This may release more $\text{Fe}^{2+} \leftrightarrow \text{Fe}^{3+}$ space charge. Later at higher content of LiAl, a new magnetic order may commence due to the affinity of lithium towards iron. This will restrict the mobility of $\text{Fe}^{2+} \leftrightarrow \text{Fe}^{3+}$ space-charge.

3.2 Relaxation spectra :

In order to obtain more information on space-charge the relaxation spectra of the samples are also investigated. The set of two plots (i) K' v/s frequency and (ii) K'' v/s frequency, known as relaxation spectra are given in Figures 3 and 4 respectively. The nature of curves is similar to shown by Maxwell-Wagner model for space-charge [20]. From Figure 3, it is clear that the value of dielectric constant $K'_{10\text{kHz}}$ is maximum for S_{25} . Hence, it is concluded that the space-charge is maximum in sample S_{25} . The curve falls rapidly with frequency. Hence the relaxation frequency of the space-charge of S_{25} may be lower than 10kHz, but close to 10 kHz. The value of dielectric constant K' at 10 kHz

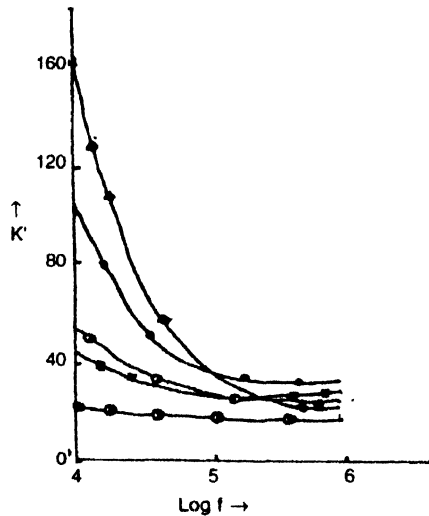


Figure 3. A relaxation spectra (dielectric constant K') of S_0 (.), S_{25} (◆), S_{50} (■), S_{75} (⊙) and S_{100} (⊗) at room temperature

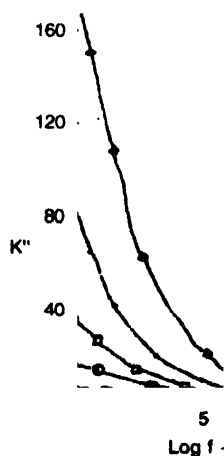


Figure 4. A relaxation spectra (dielectric loss K'') of S_0 (.), S_{25} (◆), S_{50} (■), S_{75} (⊙) and S_{100} (⊗) at room temperature.

and its subsequent fall with frequency is somewhat less in case of S_{00} . This implies that space-charge as well as its relaxation frequency in S_{00} are less than in S_{25} . For the remaining three samples, the space-charge is observed to be very small.

It is clear from Figure 4 that K'' is the largest for S_{25} . Therefore, the largest conductivity term corresponds to S_{25} . The conductivity term corresponding to S_{00} is smaller than that corresponding to S_{25} . The conductivity terms are much smaller for remaining samples.

3.3 Variation of dielectric constant (K') with temperature at 1 kHz :

Further, the variation of K' with temperature (from 300 K to 650 K) is investigated to find if there exists ferroelectric/diffused phase or any other transition. The variation of K' with temperature is shown in Figure 5 for all the samples. The curve corresponding to S_{00} shows that K' increases slowly from 300 K. It shows discontinuity at 500 K and increases rather rapidly from 500 K. It is interesting to note that the discontinuity at 500 K agrees with antiferro to paramagnetic transition [9]. Hence, it is concluded that above 500 K $\text{Fe}^{2+} \leftrightarrow \text{Fe}^{3+}$ space-charge becomes available in the large quantity and therefore, the dielectric constant (K') increases, rapidly above 500 K. In comparison, the curves corresponding to other samples are rather well separated from the curve belonging to S_{00} . The dielectric constants of the other samples remain almost constant from 300 to 550 K. Beyond 550 K their dielectric constants increase rather slowly. It is interesting to note that the transition around 550 K in the other sample is rather broad. This implies that a pretransition magnetic order is weak as in the case of S_{00} .

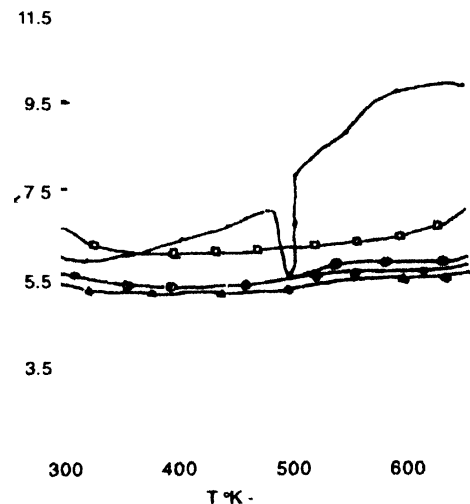


Figure 5. A plot of dielectric constant (K') vs temperature.

The overall lowering of the space-charge in the remaining samples may be attributed to the following possibilities

- (i) $(\text{LiAl})^{4+}$ replaces Ti^{4+} ,
- (ii) Li is known for its affinity towards octahedral sites and iron,

- (iii) Li^{1+} may act as an acceptor as shown in Figure 6. This may eliminate presence of Fe^{2+} ions at least partly.

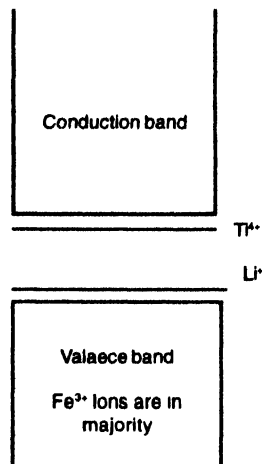


Figure 6. Li^{+} acts an acceptor.

3.4 Conductivity at 1MHz at room-temperature :

In order to elaborate the role of "LiAl" pair, the d.c. conductivities of the samples are measured at room temperature. They are shown in Table 2.

Table 2. Data showing effective carrier concentration, room temperature conductivity and particle size

Sample	S_{00}	S_{25}	S_{50}	S_{75}	S_{100}
Concen. of donors	0.33	0.23	0.13	0.03	0.00
Concen. of acceptors	0.00	0.20	0.40	0.60	0.66
Effe. Carrier	0.33	0.03	0.27	0.57	0.66
Concen. and type	(n)	(n)	(p)	(p)	(p)
D. C. Conductivity $\times 10^{-4}$ mho/m	3.45	2.07	4.20	6.10	14.00
Ple. size \AA	337	375	646	585	423
Assumed cation distribution on 4c site					
S_{00} - $\text{Fe}_{0.67}\text{Ti}_{0.33}$					
S_{25} - $\text{Fe}_{0.67}\text{Ti}_{0.23}(\text{LiAl})_{0.10}$					
S_{50} - $\text{Fe}_{0.67}\text{Ti}_{0.13}(\text{LiAl})_{0.20}$					
S_{75} - $\text{Fe}_{0.67}\text{Ti}_{0.03}(\text{LiAl})_{0.40}$					
S_{100} - $\text{Fe}_{0.67}\text{Ti}_{0.00}(\text{LiAl})_{0.66}$					

Since the internal fields due to dipolar and interfacial polarization are insignificant, therefore, the conductivity is only due to electronic conduction. Supposing that the $(\text{LiAl})^{4+}$ replaces Ti^{4+} on, say, 4c site. The carrier concentration and its nature is determined as in Table 2. These values are compared with the conductivities (Figure 7). The linearity of the plot means that σ is directly proportional to carrier concentration. This suggests that, most of the $(\text{LiAl})^{4+}$ substitutes Ti^{4+} on 4c site.

The substitution will be mainly on the grain boundary which will affect the grain growth. Hence, any deviation from this linear relationship will be mainly due to the particle size as can be seen from Table 2 [21]. However, mobility and substitution on 8f sites

may also be minor contributors to the deviation from linearity. Therefore, it is concluded that Li acts as a dopant (acceptor), and compensates 'n' impurity. Also, it is concluded a 'LiAl' pair substitutes Ti mainly on the grain boundary, alters grain growth. Hence, doping, impurity, compensation and grain texture are responsible for changes in the resistivities, dielectric constant and dielectric loss in the samples.

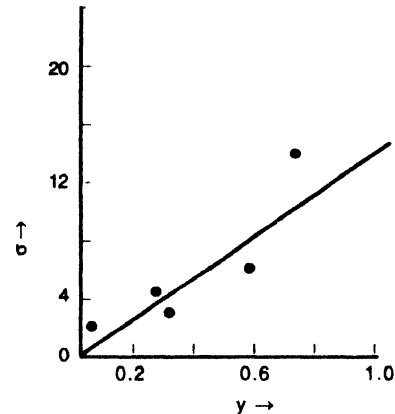


Figure 7. A plot of carrier concentration (Y) vs conductivity (σ) at room temperature

References

- [1] S Akimoto, T Nagata and T Katsura *Nature* **37** 179 (1957)
- [2] E Gurewitz and U Atzmony *Phys. Rev.* **B26** 6093 (1982)
- [3] R S Singh, T H Ansari, R A Singh, B M Wanklyn and B E Watt *Solid State Commun* **94** 1003 (1995)
- [4] J K Srivastava, J Hammann, K Asai and K Katsumata *Phys. Lett. A* **149** 485 (1990)
- [5] J K Srivastava, S Morimoto and A Ito *Hyperfine Inter* **54** 717 (1990)
- [6] R L Lichti, S Kumar and C Bockema *J. Appl. Phys.* **63** 4351 (1988)
- [7] J L Tholence, Y Yeshurum and B Wanklyn *Solid State Phys.* **19** 235 (1986)
- [8] K Iwauchi and Y Ikeda *Phys. Stat. Sol.* **119** K71 (1990)
- [9] U Atzmony, E Gurewitz, M Melamud, H Pinto, H Shamed, G Gorodetsky, E Herum, R M Horreich, S Shtrikman and B Wanklyn *Phys. Rev. Lett.* **43** 782 (1979)
- [10] S W Poulik, M H Zimmerman, K T Faber and F R Fuller (Jr) *J. Mater. Res.* **11** 2795 (1996)
- [11] Gunner Eriksson, A D Petton, E Woermann and A Ender *Ber. Bun. Phys. Chem.* **100** 1839 (1996)
- [12] M H Zimmermann, K T Faber, E R Fuller, K L Jr. Kruger and K J Bowman *J. Am. Ceram. Soc.* **79** 1389 (1996)
- [13] M Drogenik, L Golic, D Hanzel, V Krasevec, A Prodan, M Bakker and D Kolar *J. Solid State Chem.* **40** 47 (1981)
- [14] D Cordischi, N Burriesci, F D'Alba, M Petrera, G Polizzotti and M Schiavello *J. Solid State Chem.* **56** 182 (1995)
- [15] D S Ginley and M A Butler *J. Appl. Phys.* **48** 2019 (1977)
- [16] D S Ginley and R J Boughman *Mater. Res. Bull.* **11** 1539 (1976)
- [17] T R Mc Guire and F S Ferebee *J. Appl. Phys.* **34** 1821 (1963)
- [18] Jie Chem, M Chan Helen and P Harner Martin *J. Am. Ceram. Soc.* **72** 593 (1989)
- [19] K Uchino and S Namura *Ferro. Lett.* **44** 56 (1983)
- [20] A R Von Hippel *Dielectric and Waves* (N. Y. : Wiley) (1959)
- [21] B D Cullity *X Ray Diffraction* (Addison-Wesley) (1967)